

# Dark matter search experiment with CaF<sub>2</sub>(Eu) scintillator at Kamioka Observatory

Y. Shimizu<sup>a,\*</sup>, M. Minowa<sup>a,b</sup>, W. Suganuma<sup>a 1</sup>, Y. Inoue<sup>c</sup>

<sup>a</sup>*Department of Physics, School of Science, University of Tokyo, 7-3-1,  
Hongo, Bunkyo-ku, Tokyo 113-0033, Japan*

<sup>b</sup>*Research Center for the Early Universe(RESCEU), School of Science, University  
of Tokyo, 7-3-1, Hongo, Bunkyo-ku, Tokyo 113-0033, Japan*

<sup>c</sup>*International Center for Elementary Particle Physics(ICEPP), University of  
Tokyo, 7-3-1 Hongo, Bunkyo-ku, Tokyo 113-0033, Japan*

---

## Abstract

We report recent results of a WIMP dark matter search experiment using 310g of CaF<sub>2</sub>(Eu) scintillator at Kamioka Observatory. We chose a highly radio-pure crystal, PMTs and radiation shields, so that the background rate decreased considerably. We derived limits on the spin dependent WIMP-proton and WIMP-neutron coupling coefficients,  $a_p$  and  $a_n$ . The limits excluded a part of the parameter space allowed by the annual modulation observation of the DAMA NaI experiment.

*Key words:* Scintillation detector, Calcium fluoride, Dark matter, WIMP

*PACS:* 14.80.Ly, 29.40.Mc, 95.35.+d

---

<sup>1</sup> Now at Third Research Center, Technical research and Development Institute, Japan Defence Agency, 1-2-10, Sakae, Tachikawa, Tokyo 190-8533, Japan

\* Corresponding author.

*Email address:* pikachu@icepp.s.u-tokyo.ac.jp (Y. Shimizu).

## 1 Introduction

There is substantial evidence that most of the matter in our Galaxy must be dark matter that exists in the form of Weakly Interacting Massive Particles (WIMPs) [1]. WIMPs are thought to be non-baryonic particles, and the most plausible candidates for them are the lightest supersymmetric particles. WIMPs can be directly detected through elastic scattering with nuclei in radiation detectors. Using various detectors, many groups have performed experiments for the detection of WIMPs.

For the direct WIMP detection, two kinds of interactions need to be considered: the axial-vector (Spin-Dependent, SD) interaction and the scalar (Spin-Independent, SI) interaction. WIMPs couple to the spin of the target nuclei in the SD interaction while they coherently couple to almost all nucleons of the target nuclei in the SI interaction. For the SD interaction,  $^{19}\text{F}$  is one of the most favorable nuclei to detect WIMPs because of its large nuclear spin and 100% natural abundance. Furthermore, the spin expectation values of protons and neutrons in  $^{19}\text{F}$  have the opposite signs while those values in other nuclei usually have the same signs [2–6]. Therefore, experiments with a  $^{19}\text{F}$ -target can set complementary limits to those with nuclei whose spins have the same sign.

Several direct WIMP searches using  $^{19}\text{F}$ -based detectors, such as bolometers [7,8], scintillators [9,10] and superheated droplet detectors (SDDs) [11,12], have already been performed. Our group had also carried out WIMP search experiments using LiF and NaF bolometers [7,8]. Although these results set complementary limits to those of NaI(Tl) experiments, the background rates below 20 keV could not be decreased sufficiently. The sources of the main background were thought not to be any radiation but to be intrinsic and instrumental noises in the bolometers. As an alternative method, we have carried out experiments using  $\text{CaF}_2(\text{Eu})$  scintillators.  $\text{CaF}_2(\text{Eu})$  is known as a useful scintillator for WIMP searches because of its high light yield (19000 photons/MeV) and has already been used in several experiments. However, these experiments show rather high background rates ( $\gtrsim 10$  counts/k.e.e./day/kg<sup>2</sup>) in comparison with the NaI(Tl) experiments ( $\sim 1$  counts/k.e.e./day/kg). In addition, its light yield is about 50 % of NaI(Tl), so that the energy threshold of  $\text{CaF}_2(\text{Eu})$  detectors is higher than NaI(Tl) detectors. Therefore, these  $\text{CaF}_2(\text{Eu})$  experiments set less stringent limits to the SD interaction than the NaI(Tl) experiments. In order to reduce the background rates and to improve the energy threshold of our experiments, we have tried to eliminate radioactive

---

<sup>2</sup> In this letter, we use the unit k.e.e. or keV electron equivalent for nuclear recoil energy since the scintillation efficiency for nuclear recoils is less than electron recoils due to high ionization loss.

sources of  $\gamma$ -rays and studied detection efficiency near the energy threshold.

In this letter, the results of our new experiment with a  $\text{CaF}_2(\text{Eu})$  scintillator are presented.

## 2 Experimental setup

The detector consisted of a  $\text{CaF}_2(\text{Eu})$  crystal with a mass of 310g. It was installed in Kamioka Observatory (2700 m.w.e.). To reduce the background, low radioactive PMTs (Hamamatsu R8778) and a low radioactive radiation shield were used. The experimental setup is shown in Fig 1. The crystal was produced from the same stock of  $\text{CaF}_2$  raw powder as used by the CANDLES experiment [14] and low radioactive  $\text{EuF}_3$  powder. The low radioactive PMT was developed by the XMASS experiment [13] and thought to be the least radioactive among available PMTs. Two PMTs were attached to the crystal through 5cm-long quartz light guides. The photoelectron yield of the scintillator was about 4 photoelectrons/k.e.e. at 60 k.e.e. The radiation shield consisted of 5cm of highly pure copper (99.9999%), 10 cm of OFHC copper, 15 cm of lead, and 20 cm of polyethylene. The highly pure copper was supplied by Mitsubishi Materials. The whole setup was separated from the mine air by two layers of EVOH sheet [15] so that radon gas in the air could not come into the detector. The radon free air generated in Kamioka observatory was sent into the detector as shown in the figure. In addition, the radon concentration around the detector was continuously monitored by a radon detector. It was kept at about 30 mBq/m<sup>3</sup> throughout the experiment.

For the data acquisition, a dual trace digital oscilloscope was used to record wave forms of PMT pulses. The pulses of each PMT are directly sent to the oscilloscope without any amplifier then daisy-chained to a trigger system with a tee connector. The impedance of each oscilloscope input was set to 1M $\Omega$  and the cables are terminated at the inputs of the trigger system. The wave forms were digitized at the oscilloscope at a rate of 1 GS/s for a total digitization time of 10  $\mu$ s and sent to a PC for an off-line analysis.

In the trigger system, the pulses were amplified by PMT amplifiers and sent to low threshold discriminators. Thresholds of the discriminators were set to 1/4 of the mean pulse height of single photoelectron events. The single photoelectron events were obtained by irradiating the PMT with continuous feeble light from an LED. The detection efficiency of each PMT with the discriminator threshold for a single photoelectron event was obtained to be 0.8 by comparing the discriminator output counts and the total number of single photoelectron events; the latter was estimated by assuming a normal distribution for the charge distribution of the single photoelectron events. Parameters of the nor-

mal distributions were determined in a special measurements by recording the events with low-threshold internal triggers of the oscilloscope to include the low energy tail of the spectrum. The charge distribution of the internally triggered events was well fitted by the normal distribution. Single counting rates of PMTs were typically 20 Hz.

The discriminator signals were then sent to the coincidence circuit. It generated a trigger pulse for the oscilloscope when both of the PMTs gave signals in coincidence within  $1\mu\text{s}$ . It reduced the number of background events due to dark noise of the PMTs.

The trigger efficiency of the data acquisition system was calculated as a function of a number of photoelectrons by the Monte-Carlo analysis. In this analysis, we generated a certain number of photoelectrons in a time sequence according to the scintillation decay time of  $\text{CaF}_2(\text{Eu})$ . We assumed each photoelectron reached in each PMT evenly. The detection probability of a photoelectron was set to 0.8. Then, we measured an interval between arbitrary photoelectrons of each PMT in the event. The fraction of events that generated at least one output signal in both of the discriminators within  $1\mu\text{s}$  was taken to be the trigger efficiency. At 2 k.e.e., 8 photoelectrons were generated and the trigger efficiency was calculated to be 0.93. Threshold energy for the following analysis was set at 2 k.e.e.

### 3 Measured spectra

The WIMP observation was carried out from March to May 2005. Measured spectra are shown in Fig 5. The energy scale of the spectra is defined to be proportional to the number of photoelectrons. In the energy region below 10 k.e.e., background events due to Cherenkov photons dominate the event rates. The Cherenkov events were produced in the light guides by Compton electrons caused by background  $\gamma$ -rays. We used a pulse shape discrimination (PSD) technique to eliminate these events. Cherenkov photons are observed as fast pulses ( $< 10\text{ ns}$ ) while scintillation photons as slow pulses ( $\sim 1\mu\text{s}$ ). Therefore, we used the ratio of the integral charge of the partial pulse shape period (0–30 ns) to that of the total pulse shape period (0–10  $\mu\text{s}$ ) as a discrimination parameter in the off-line analysis. To set the discrimination cut, we compared low energy Compton events which cannot produce Cherenkov photons (obtained using 122 keV  $\gamma$ -rays from  $^{57}\text{Co}$ ) and Cherenkov events (obtained using 1133 and 1333 keV  $\gamma$ -rays from  $^{60}\text{Co}$ ). In addition, we eliminate events in which observed charge of the two PMTs shows high asymmetry because they are thought to be the remaining Cherenkov events or electric noise events. To estimate the efficiency of the off-line event selection, the low energy Compton events were used. We calculated a fraction of the events which remained after

the selection as a function of energy. It was 0.74 at 2 k.e.e. Consequently, the event selection reduced the count rates to less than 10 counts/k.e.e./day/kg in the energy region between 2 and 10 k.e.e.

#### 4 Limits on the WIMP-nucleon interaction

Using the measured spectrum, limits on the SD WIMP-nucleon interaction were derived. The limits were calculated using the same manner as described in Ref. [16]. To derive the upper limits, we conservatively assumed all events to be nuclear recoils caused by the WIMP scattering. The astrophysical and nuclear parameters used to obtain the limits are listed in Table 1. Only the contribution of  $^{19}\text{F}$  was considered while  $^{40}\text{Ca}$  had negligible contribution to the SD interaction because  $^{40}\text{Ca}$  consisted of even protons and even neutrons. The scintillation efficiency  $f_q$  of the  $^{19}\text{F}$  recoil in a  $\text{CaF}_2(\text{Eu})$  was measured by other experiments. Although all of these experiments show that the scintillation efficiency tends to increase in lower energy region, we choose conservatively a constant value  $f_q = 0.11$ . As was done in Ref. [17],  $^{19}\text{F}$  recoil energy is calculated with  $f_q$  and the interpolated energy scale between 0 and 60 k.e.e.:

$$E_N = \frac{L}{L_{60\text{keV}}} \frac{60[\text{keV}]}{f_q} \quad (1)$$

where  $E_N$  is the  $^{19}\text{F}$  recoil energy and  $L$  is the scintillation yield of an event.

For the SD interaction, the WIMP-nucleus cross section is written as

$$\sigma_{\chi-N}^{\text{SD}} = \frac{32G_F^2 \mu_{\chi-N}^2}{\pi} (a_p \langle S_{p(N)} \rangle + a_n \langle S_{n(N)} \rangle)^2 \frac{J+1}{J}, \quad (2)$$

where  $G_F$  is the Fermi coupling constant,  $\mu_{\chi-N}$  is the WIMP-nucleus reduced mass,  $\langle S_{p(N)} \rangle$  and  $\langle S_{n(N)} \rangle$  are the expectation values of the proton and neutron spins within the nucleus and  $J$  is the total nuclear spin [18].

The upper limit of the WIMP-nucleus scattering cross section  $\sigma_{\text{lim}\chi-N}^{\text{SD}}$  is obtained by the experiment. From Eq. (2), limits in the  $a_p$ - $a_n$  plane is written with  $\sigma_{\text{lim}\chi-N}^{\text{SD}}$ :

$$(a_p \langle S_{p(N)} \rangle + a_n \langle S_{n(N)} \rangle)^2 \frac{J+1}{J} < \frac{\pi \sigma_{\text{lim}\chi-N}^{\text{SD}}}{32G_F^2 \mu_{\chi-N}^2}. \quad (3)$$

As in Ref. [19], limits on a single nucleon interaction are generally calculated:

$$\begin{aligned}
\sigma_{\lim\chi-p(N)}^{\text{SD}} &= \sigma_{\lim\chi-N}^{\text{SD}} \frac{\mu_{\chi-p}^2}{\mu_{\chi-N}^2} \frac{\langle S_p \rangle^2}{\langle S_{p(N)} \rangle^2} \frac{J+1}{J}, \\
\sigma_{\lim\chi-n(N)}^{\text{SD}} &= \sigma_{\lim\chi-N}^{\text{SD}} \frac{\mu_{\chi-n}^2}{\mu_{\chi-N}^2} \frac{\langle S_n \rangle^2}{\langle S_{n(N)} \rangle^2} \frac{J+1}{J},
\end{aligned} \tag{4}$$

where  $\langle S_p \rangle = \langle S_n \rangle = \frac{1}{2}$ ,  $\sigma_{\lim\chi-p(N)}^{\text{SD}}$  and  $\sigma_{\lim\chi-n(N)}^{\text{SD}}$  are the WIMP-proton and WIMP-neutron scattering cross section limits when  $a_n \langle S_{n(N)} \rangle = 0$  and  $a_p \langle S_{p(N)} \rangle = 0$  in Eq. (3), respectively. Figure 3 shows  $\sigma_{\lim\chi-p(N)}^{\text{SD}}$  and  $\sigma_{\lim\chi-n(N)}^{\text{SD}}$  derived from our experiment as a function of WIMP mass  $M_\chi$ . Results of other experiments are also shown in the figure.

The limits in the  $a_p$ - $a_n$  plane for WIMP mass  $M_\chi = 50$  and 200 GeV are shown in Fig 4. The limits of other experiments are also shown. The outside of the two solid lines is excluded by our experiment. The region between the two ellipses is allowed by the annual modulation observation of the DAMA experiment [24]. Our results exclude a part of the DAMA allowed region by means of odd-proton target. Experiments with odd-neutron targets such as the CDMS [21] also set similar limits. Our results are comparable to the recent results of PICASSO [12] experiment which uses SDDs of fluorocarbon,  $C_4F_{10}$ .

## 5 Conclusion

The WIMP search experiment using 310g of  $CaF_2(Eu)$  was carried out. The highly pure copper shield and the quartz light guides were used to eliminate  $\gamma$ -rays from the outer materials. Pulse shape discrimination effectively eliminated Cherenkov events, which dominated the count rates below 10 k.e.e. As a result, count rates were lower than 10 counts/k.e.e./day/kg between 2 and 10 k.e.e. We obtained the limits on the WIMP-nucleon spin dependent interaction in terms of the WIMP-nucleon coupling coefficients  $a_p$  and  $a_n$ . Our results excluded a part of the parameter region allowed by the annual modulation measurement by the DAMA NaI experiment.

## Acknowledgements

We would like to acknowledge the help of the staff of Kamioka Observatory, Institute for Cosmic Ray Research, University of Tokyo in performing this experiment. We want to express our thanks to XMASS collaboration for allowing us to obtain the low radioactive PMT R8778 based on their development. We also want to express our thanks to Prof. T. Kishimoto of CANDLES collaboration for allowing us to obtain the low background  $CaF_2(Eu)$  crystal based

on the low background CaF<sub>2</sub>(pure) they developed. This research is supported by Research Center for the Early Universe, School of Science, University of Tokyo.

## References

- [1] G. Jungman, M. Kamionkowski and K. Griest, Phys. Rep. **267** (1996) 195.
- [2] J. Engel, S. Pittel, E. Ormand and P. Vogel, Phys. Lett. B **275** (1992) 119.
- [3] J. Engel, S. Pittel and P. Vogel, Int. J. Mod. Phys. E **1** (1992) 1.
- [4] M. T. Ressell *et al.*, Phys. Rev. D **48** (1993) 5519.
- [5] J. Engel *et al.*, Phys. Rev. C **52** (1995) 2216.
- [6] M. T. Ressell and D. J. Dean, Phys. Rev. C **56** (1997) 535.
- [7] K. Miuchi *et al.*, Astropart. Phys. **19** (2003) 135.
- [8] A. Takeda *et al.*, Phys. Lett. B **572** (2003) 145.
- [9] R. Bernabei *et al.*, Astropart. Phys. **7** (1997) 73; R. Belli *et al.*, Nucl. Phys. B **563** (1999) 97.
- [10] I. Ogawa *et al.*, Nucl. Phys. A **663** (2000) 869c.
- [11] F. Giuliani *et al.*, Phys. Lett. B **588** (2004) 151.
- [12] M. Barnabe-Heider *et al.*, Preprint hep-ex/0502028.
- [13] S. Moriyama *et al.*, Proc. of International Workshop on Technique and Application of Xenon Detectors (Xenon01) (World Scientific, 2001).
- [14] S. Yoshida *et al.*, Nucl. Phys. B (Proc. Suppl.) **138** (2005) 214. S. Umehara *et al.*, to be published in the Proceedings of Symposium on Neutrino and Dark Matters in Nuclear Physics (NDM03).
- [15] <http://www.kuraray.co.jp/en/index.html>.
- [16] J. D. Lewin and P. F. Smith, Astropart. Phys. **6** (1996) 87.
- [17] D. R. Tovey *et al.*, Phys. Lett. B **433** (1998) 150.
- [18] J. Ellis *et al.*, Phys. Lett. B **481** (2000) 304.
- [19] D. R. Tovey *et al.*, Phys. Lett. B **488** (2000) 17.
- [20] B. Ahmed *et al.*, Astropart. Phys. **19** (2003) 691.
- [21] D. Akerib *et al.*, Phys. Rev. Lett. **93** (2004) 211301.
- [22] R. Bernabei *et al.*, Phys. Lett. B **509** (2001) 197.
- [23] R. Bernabei *et al.*, Phys. Lett. B **436** (1998) 379.
- [24] F. Giuliani and TA Girard, Phys. Rev. D **71** (2005) 123503.

Astrophysical parameters	
Dark matter density	0.3 GeV/cm <sup>3</sup>
Velocity distribution	Maxwellian
Velocity dispersion	220 km/s
Solar system velocity	232 km/s
Nuclear parameters of <sup>19</sup> F	
Total spin	$\frac{1}{2}$
Spin expectation value of protons	0.441
Spin expectation value of neutrons	-0.109

Table 1  
Astrophysical and nuclear parameters used to obtain the limits.

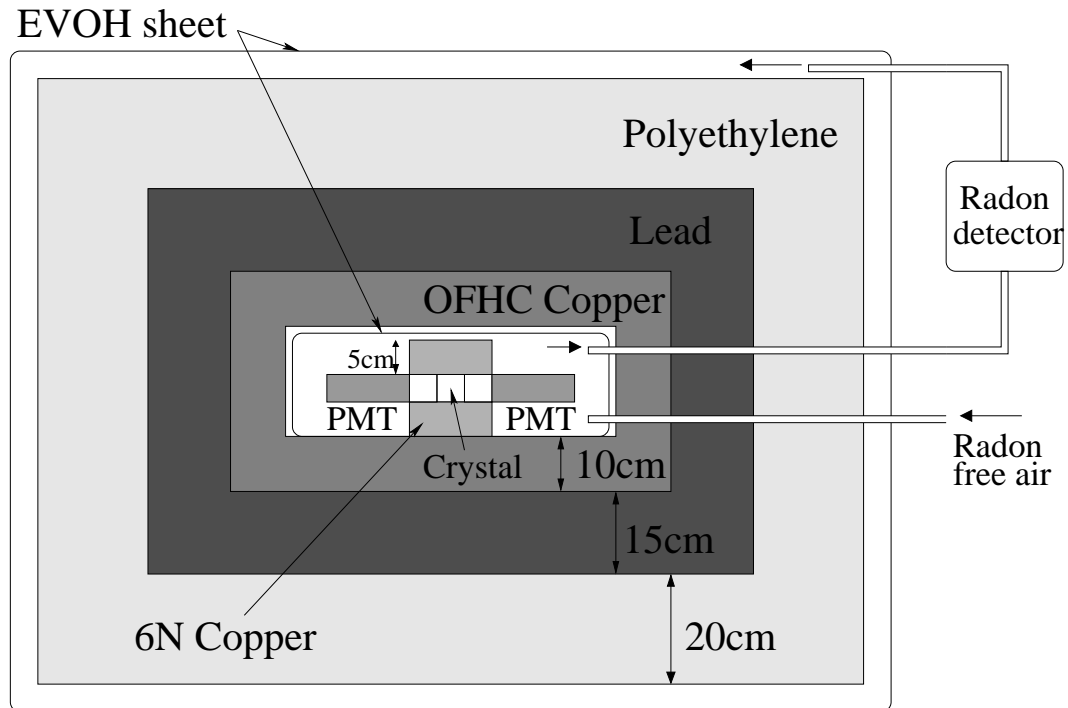


Fig. 1. Schematic view of the experimental setup.



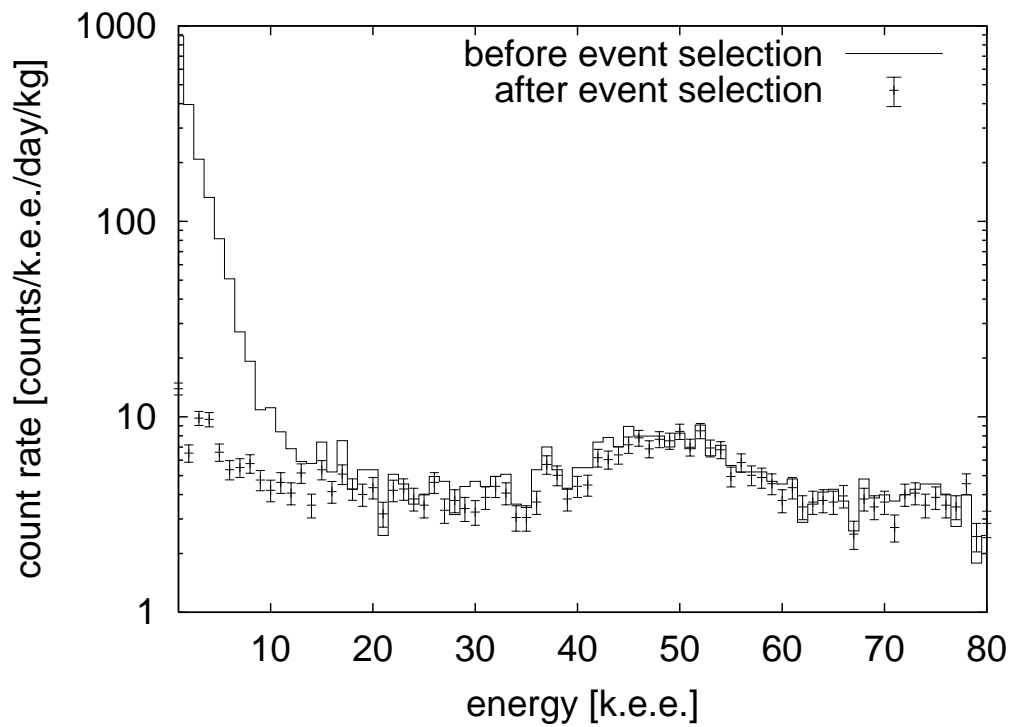


Fig. 2. Measured spectra before and after the event selection is applied. The energy scale is normalized to a calibration point of 60 keV electron recoil.

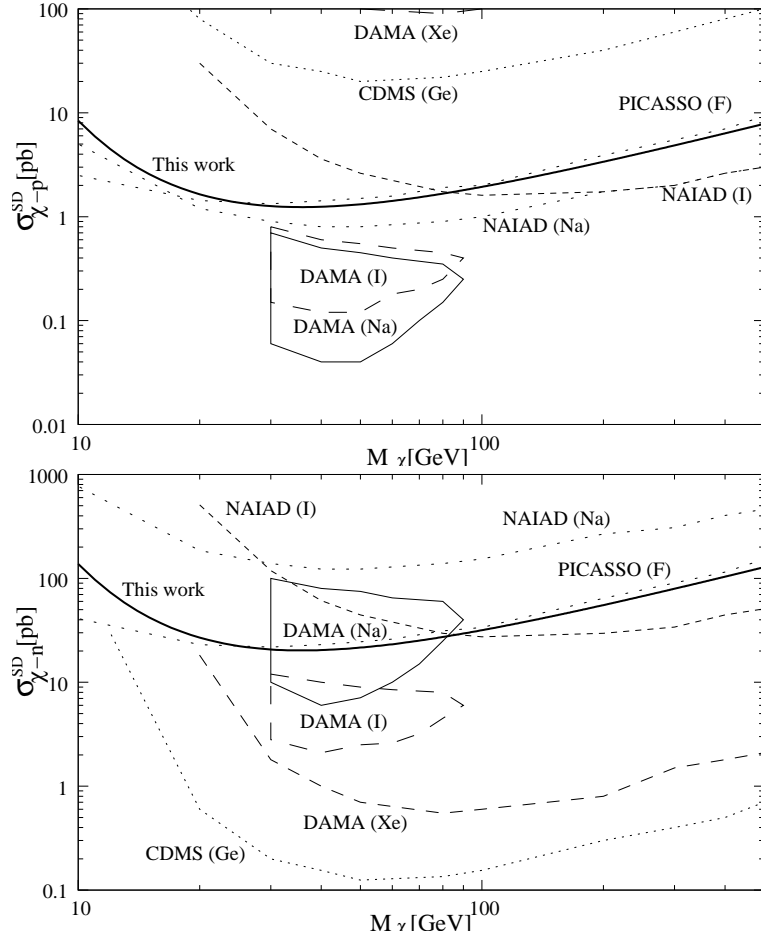


Fig. 3. Recent limits on the SD WIMP-proton cross section and WIMP-neutron cross section. Results of NAIAD[20], PICASSO[12], CDMS[21], DAMA NaI[22], DAMA Xe[23] and our experiments are shown.

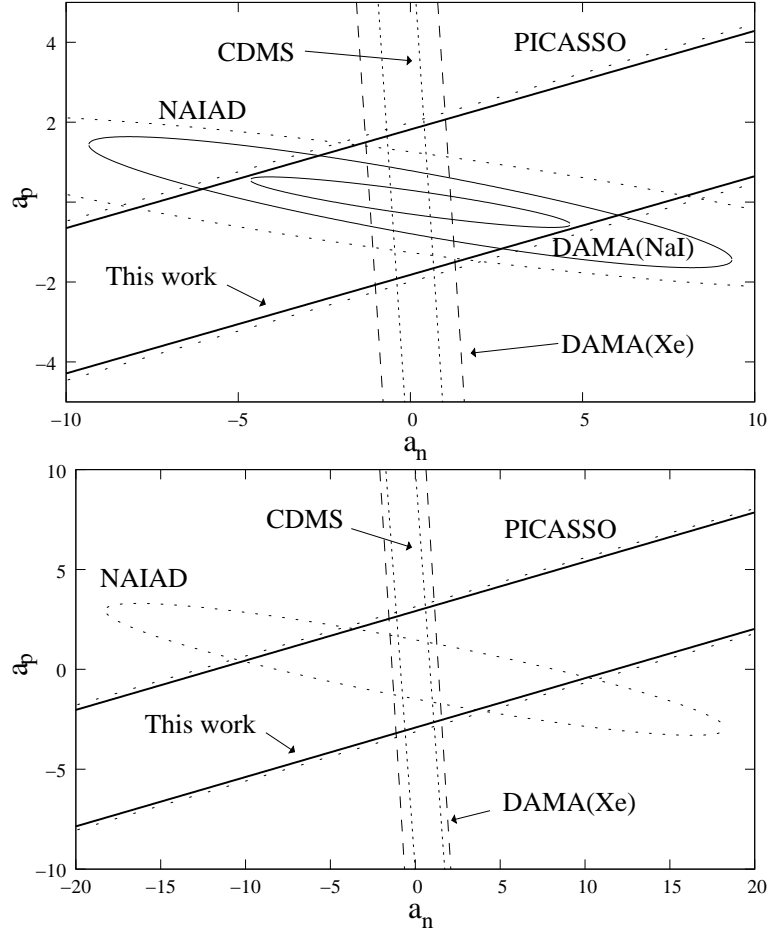


Fig. 4. Limits in the  $a_p$ - $a_n$  plane for  $M_\chi = 50$  GeV (upper) and 200 GeV (lower). The region between two solid lines is allowed by this experiment. Results of NAIAD[20], PICASSO[12], CDMS[21], DAMA NaI[22] and DAMA Xe[23] experiments are also shown.